Oxidation of designed model peptides containing methionine, proline and glutamic acid investigated by tandem mass spectrometry and IRMPD spectroscopy

Yining Jiang, Jean-Xavier Bardaud, Nouha Ayadi, Marc Lecouvey, Chantal Houée-Levin, Giel Berden, Jos Oomens, Debora Scuderi

International Journal of Mass Spectrometry 487 (2023) 117029

Contents lists available at ScienceDirect

International Journal of Mass Spectrometry

journal homepage: www.elsevier.com/locate/ijms

Oxidation of designed model peptides containing methionine, proline and glutamic acid investigated by tandem mass spectrometry and IRMPD spectroscopy

Yining Jiang [a], Jean-Xavier Bardaud [a, b], Nouha Ayadi [c], Marc Lecouvey [c], Chantal Houée-Levin [a], Giel Berden [d], Jos Oomens [d, e], Debora Scuderi [a, *]

[a] Université Paris-Saclay, CNRS, Institut de Chimie Physique, UMR8000, 91405, Orsay, France
[b] LIDYL, CEA, CNRS, Université Paris-Saclay CEA Saclay, Bât 522, Gif-sur-Yvette, 91191, France
[c] Department of Chemistry, Université Sorbonne Paris Nord, CSPBAT, CNRS, UMR 7244, 1 rue de Chablis, Bobigny, F-93000, France
[d] Radboud University, Institute for Molecules and Materials, FELIX Laboratory, Toernooiveld 7, Nijmegen, 6525 ED, Netherlands
[e] Van't Hoff Institute for Molecular Sciences, University of Amsterdam, P.O. Box 94157, Amsterdam, 1090 GD, Netherlands

ARTICLE INFO

Article history:
Received 29 December 2022
Received in revised form
17 February 2023
Accepted 25 February 2023
Available online 27 February 2023

Keywords:
One-electron oxidation
Tandem mass spectrometry
IRMPD spectroscopy

ABSTRACT

Oxidation by OH radicals produced by γ-radiolysis of single amino acids proline and glutamic acid accompanied by a series of Met-containing model peptides were investigated by a combined study of tandem mass spectrometry and infrared multiple-photon dissociation spectroscopy in the fingerprint region. The thioether group of methionine has been identified as a common target of OH free radicals leading to a S^+ radical cation, which made a 2-center-three electron (2c-3e) bond with any atom having having a lone pair of electrons. However, the final fate of these 2c-3e free radicals is still unknown. These studies led to the identification of the final stable products of oxidation and the localization of the modified sites. We show that the final products contain mostly methionine sulfoxide, whatever the structure of the preceding free radical. Although the distance between two Met residues controls the nature of free radicals formed in the peptides, it has no significant effect on the final products of oxidation. These results thus confirm that the final products are not controlled by free radical structure. Also, although no proline free radical was detected previously, we show that proline residue can be oxidized.

1. Introduction

Methionine (Met) is an essential amino acid in the metabolism of many living organisms including humans [1,2]. Due to the presence of the thioether functional group on its side chain, Met is one of the main targets of oxidation residues in proteins. Its oxidation can cause dysfunction of proteins and lead to undesired diseases, e.g., Alzheimer's disease [3–5], and cellular aging [6–8]. Met residue can also act as a molecular switch to detoxify antioxidants and thus protect important regions of the proteins [9]. The first steps of Met one-electron oxidation induced by OH radicals involve transients that have been characterized by pulse radiolysis [10–12]. Two competitive pathways were shown: direct $^{\bullet}$OH addition on the S-atom and H-atom elimination from α-S position. In the former, a S-centered radical cation (>$S^{+\bullet}$) is formed. It can be stabilized by a 2-center-3-electron (2c-3e) bond with any atom having a lone pair, e.g. (S ∴ S), (S ∴ N), and (S ∴ O). In the latter, a carbon-centered radical is observed. The nature of the 2-center-three electron (2c-3e) bonded intermediates depends on the structural, geometrical, and conformational properties of the peptide [13]. The impact of the free radical structure on final products is still not well investigated.

Oxidation of peptides containing Methionine (M), Proline (P) and/or Glutamic acid (E) has been investigated by pulse radiolysis. Only free radicals coming from methionine were detected [14,15], suggesting that the other residues were protected from oxidation. Indeed the rate constants of oxidation by OH radicals with these residues are in favor of reactions with methionine mostly ($k(OH + Met) = 8.5 \times 10^9$ $Mol^{-1}.L.s^{-1}$; $k(OH + Pro) = 3.1 \times 10^8$ $Mol^{-1}.L.s^{-1}$; $k(OH + Glu) = 2.3 \times 10^8$ $Mol^{-1}.L.s^{-1}$) [16].

* Corresponding author.
E-mail address: debora.scuderi@u-psud.fr (D. Scuderi).

https://doi.org/10.1016/j.ijms.2023.117029
1387-3806/

Previous pulse radiolysis studies have also shown that Pro residues did not serve as electron transfer bridge but could modulate the peptide folding and hence act on the decarboxylation process [13,17]. Designed model peptides with variable-length proline bridges have been investigated in this work, namely Met-$(Pro)_n$-Met (n = 1 or 2), to understand the effects of different factors on the final oxidation products in peptides containing methionine. The use of such peptides allows for distance control between the sulphur atoms located in the side chains of Met residues. Such an approach can help to study the eventual existence of long-range Electron Transfer (ET) between amino acid residues on final products formed in the oxidation process. Additionally, the effect of possible intramolecular contact formation in the stabilisation of the sulphur-centered radical cation formed during γ-radiolysis in γ-Glu-Pro-Met has been investigated as well, where the N-terminal Met was replaced by γ-Glu.

Pro is an important amino acid which plays a key role in collagen biosynthesis [18], as an antimicrobial agent [19] and in interaction between proteins through poly-Pro regions. A therapeutic action of Pro-Met peptides against the dengue virus was demonstrated [20,21]. In contrast to other amino acids, relatively little attention has been devoted to the radiolysis of proline [22–24]. However, in view of the high content of proline in collagen and elastin that form the main components of the connective tissues, it is quite useful to get some detailed information on the radiation chemistry of isolated proline or Met-Pro et Pro-Met dipeptides as well.

2. Materials and methods

2.1. Materials

The corresponding chemical structures of the investigated amino acids and peptides are reported in Fig. 1. Proline (Pro or P) and glutamic acid (Glu or E) were purchased from Sigma Aldrich. MP, PM were purchased from BACHEM. EM, MPM, EPM and MPPM were synthesized in the group of Prof. M. Lecouvey in University Sorbonne Paris Nord, France. The process of the synthesis is described in Figure SI1. All chemical products were used without further purification.

A baffling range of peptide coupling reagents and methods were developed for the synthesis of many challenging peptide sequences [25]. Carbodiimide, in particular, was very commonly used as a carboxyl group activator for the formation of a peptide bond. Based on the literature, the synthesis of the majority of our peptide sequences was carried out from commercially available amino acids using carbodiimide hydrochloride in the presence of HOBT to minimize racemization according to a classical solution-phase technique [26].

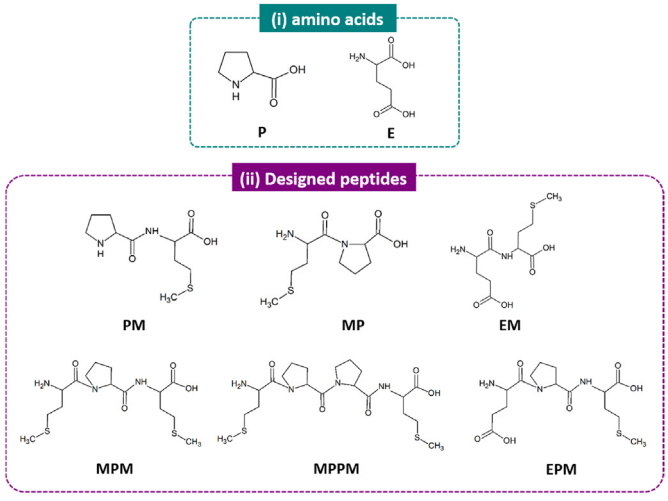

Fig. 1. Chemical structures of neutral amino acids and investigated peptides.

To eliminate the different reagents used, peptides were washed with citric acid solution, $NaHCO_3$ solution and a saturated solution of NaCl before being engaged in the deprotection step. The latter was performed, first of all, by engaging the peptides with a combination of 95% TFA, 2.5% Triethylsilane and 2.5% water and then with NaOH (1 M) solution in a mixture of THF and MeOH.

Synthesized products were used without further purification. All solvents and employed gas were of analytical grade. Deionized water was collected from a Millipore system.

2.2. Gamma source (γ) radiolysis

Samples were dissolved in ultra-pure water at a concentration of 10^{-3} M for γ-irradiation. Prior to irradiation, samples were purged by bubbling with N_2O (nitrous oxide was delivered by ALPHA GAZ. with a global purity of 99.998%) for 30 min to increase the final $^{\bullet}OH$ yield and suppress the highly reductant e^-_{aq}, according to the reaction:

$$e^-_{aq} + N_2O + H_2O \rightarrow {}^{\bullet}OH + OH^- + N_2$$

The rate constant of this reaction has been determined to be $(9.1 \pm 0.2) \times 10^9\ M^{-1}s^{-1}$ [27,28], which doubles the yield of $^{\bullet}OH$ compared to the condition without the intervention of N_2O.

In order to initiate hydroxyl-induced oxidation, γ-irradiation was carried out by using the panoramic ^{60}Co γ-source IL60PL Cis-Bio International (France) in Paris-Saclay University (Institute of Physical Chemistry, Orsay, France). The dose rate of the gamma source was determined by Fricke dosimetry and was equal to 25.45 Gy min^{-1} [29] and then corrected by the decay of the source over time. All irradiations were performed at room temperature.

In the radiation process, the relevant reaction equation is as follow [30]:

$$\mathbf{H_2O} \rightarrow (0.28)\mathbf{{}^{\bullet}OH},\ (0.062)\ \mathbf{{}^{\bullet}H},\ (0.28)\mathbf{e^-_{aq}},\ (0.047)\mathbf{H_2},\ (0.073)\mathbf{H_2O_2},\ (0.28)\mathbf{H_3O^+}$$

The chemical yields of each species after radiolysis are detailed in brackets in μM/J (known as G-values).

2.3. FT-ICR MS^2-CID analysis

The irradiated samples were diluted in 50/50 water/methanol containing 0.1% formic acid to a concentration of 100 μM. Non-irradiated solutions (with the same molecules dissolved in water and purged with N_2O) at the same concentration were employed as a reference. A 7 T hybrid FT-ICR mass spectrometer (APEX-Qe Bruker), in Orsay, France, has been used to identify all the species generated in the irradiated solution [31].

The peptides were delivered into gas-phase by an electrospray ionization (ESI) source with a flow rate of 120 μL h^{-1} and they were investigated in positive mode. Typical extraction voltage was −4500 V and the desolvation temperature was 200 °C. The dry gas flow was fixed at 8 L min^{-1} and the nebulizer pressure was set to 1.5 bar. Ions were accumulated, transferred through ion transfer optics, thermalized in a quadrupole-hexapole (Qh) interface and later extracted out towards the FT-ICR cell which is maintained under high vacuum ($<10^{-9}$ mbar) at room temperature. Mass spectra of the species were then recorded with an appropriate accumulation time depending on the abundance of interested

species, typically 1 s. Collision induced dissociation (CID-MS^2) experiments were performed in the hexapole interface by using Argon as collisional gas. The fragments were pulse-extracted and detected in ICR cell.

2.4. IRMPD spectroscopy

IR multiple photon dissociation (IRMPD) is a process that involves the successive absorption of multiple photons, the dispersion of energy in the molecule by intramolecular vibrational energy redistribution (IVR) phenomena [32], and the wavelength-specific cleavage of the molecule after exceeding the fragmentation threshold. The fragmentation channels are activated only when the IR-wavelength is in resonance with an IR vibrational mode of molecular structure [33,34].

IRMPD spectroscopy experiments have been carried out at the Free Electron Laser For Infrared eXperiments (FELIX) laboratory in Nijmegen (The Netherlands) where a Bruker AmaZon quadrupole (QIT) ion trap mass spectrometer (MS) [35,36] is coupled to the beam line of the infrared free-electron laser FELIX [37]. The QIT MS is equipped with an ESI source pumped by an external syringe pump. Ions are infused at a rate of 120 μL/h, assisted by a pressurized nebulizing gas N_2 which is heated to 200 °C. The spray voltage is of 3–5 kV. The ring electrodes of the QIT has been modified by drilling two ⌀~3 mm holes in the top-center and the bottom-center, allowing the FELIX FEL beam to enter the ion trap, interact with the ion cloud, and conduct laser spectroscopy [35].

Infrared spectra of mass-to-charge isolated ions were recorded in the 800-1900 cm^{-1} range by recording the IR photofragmentation yield after irradiating the ions with a single FEL macropulse (50–150 mJ/pulse). The FELIX IR-FEL laser produces 5–10 μs long macropulses at repetition frequency of 10 Hz. Each macropulse contains a train of ~5 ps long micropulses at a repetition rate of 1 GHz. The spectral bandwidth (FWHM) is ~0.5% of the central wavelength ($\frac{\Delta\lambda}{\lambda} = 0.5\%$). In order to prevent excessive depletion of the parent ions (saturation) and to minimize formation of fragment ions below the low mass cut-off of the QIT MS, IR spectra were recorded at several levels of laser pulse energy using a set of four attenuators [38]. Resonant absorption at characteristic wavenumbers relies strongly on molecular structures, which leads to an increase in internal energy and ends with molecular dissociation. The IRMPD spectra were obtained by plotting $-\ln\left(\frac{P}{F+P}\right)$ as a function of the IR wavenumber, where P represents the intensity of the parent ions and F the sum of the intensities of all fragment ions. The IRMPD intensity was linearly corrected for the frequency-dependent variation in laser pulse energy. The IR wavelength was calibrated with a grating spectrometer.

2.5. DFT calculations

The oxo forms of Proline and Glutamic acid were optmised at B3LYP/6–311+g(d,p) level of theory. Density function calculations were carried out using Gaussian 16 package [41]. The IR absorption spectra were computed at the same level of theory and convoluted with a Lorentzian profile (20 cm^{-1} FWHM). To account for anharmonicity, the calculated harmonic frequencies were uniformly scaled by 0.97.

3. Results and discussion

Pro (P), Glu (E) and Met (M) are the fundamental amino acids of the designed peptides. The mass spectra of the non-irradiated and γ-irradiated Pro and Glu solutions in a N_2O atmosphere are shown in Figure SI2. The most intense peaks at *m/z* 116 and 148 in the mass spectra of Pro and Glu solutions are assigned to the protonated $[P(H)]^+$ and $[E(H)]^+$, respectively. Singly ($[P(H)]^+$+16 Da) and doubly ($[P(H)]^+$+32 Da) oxidized products, at *m/z* 132 and *m/z* 148, were observed in the irradiated solution of Pro compared to the non-irradiated solution. In the mass spectra of the irradiated Glu solution, only the singly oxidized product at *m/z* 164 was detected.

The main fragments observed in the CID-MS^2 mass spectra of $[P(H)]^+$ and $[P(O)H]^+$ are reported in Table SI1. The corresponding CID-MS^2 spectra are displayed in Fig. 2. The CID-MS^2 fragmentation channel of $[P(H)]^+$ corresponds to the loss of H_2O and CO molecules, as previously observed [39]. A supplementary fragment at *m/z* 68 is observed for $[P(O)H]^+$ and can be assigned to the loss of a second H_2O molecule, indicating that the addition of the oxygen atom during the oxidation process leads to the formation of the hydroxyproline.

The main fragments observed in the CID-MS^2 spectra for $[E(H)]^+$ and $[E(O)H]^+$ are reported in Table SI2. The corresponding CID-MS^2 spectra are shown in Figure SI3. Two fragments are observed for $[E(H)]^+$ at *m/z* 130 and 102, respectively. The fragment at *m/z* 130 corresponds to the loss of a H_2O molecule. The one at *m/z* 102 is assigned to the successive loss of a H_2O and a CO molecule. $[E(O)H]^+$ shows only one fragment, which corresponds to the loss of a H_2O molecule from the oxidized amino acid.

The IRMPD spectra of the protonated oxidized forms of proline and glutamic acid have been reported in Fig. 3 and compared with the IRMPD spectra of the non-oxidized amino-acids [40,41].

The IRMPD spectra of commercial 3-hydroxyproline and 4-hydroxyproline have already been published previously [39,42].

Four major bands were observed in the IRMPD spectrum of $[P(O)H]^+$ at 1147 cm^{-1} (intense), 1347 cm^{-1} (medium), 1561 cm^{-1} (medium) and 1762 cm^{-1} (intense), consistent with that of protonated 4-hydroxyproline reported by Acharya et *al.* [39] and by Crestoni et *al.* [42]. This confirms that $[P(O)H]^+$ formed during the oxidation of Pro by gamma radiolysis leads to the formation of the hydroxyproline. Following Crestoni et *al.* [42], the intense band at 1147 cm^{-1} corresponds to the prominent band predicted at 1167-1169 cm^{-1}, assigned to the C–O stretching and COH bending modes; the medium band at 1347 cm^{-1} is the diagnostic signature of 4-hydroxyproline, attributed to NH_2 wagging predicted at 1332 cm^{-1}; and the intense band at 1762 cm^{-1} is in good agreement with the band at 1770 cm^{-1}, assigned to the carbonyl stretching mode [40]. Even if the spectrum of protonated Pro+16 shows all the spectral features of protonated (2S,4S)-4-hydroxyproline, we cannot exclude the possibility that in our experimental conditions hydroxyproline is a mixture of 4(R)- and 4(S)-hydroxyproline. More spectroscopic features are observed in the IRMPD spectrum of $[P(O)H]^+$ which we recorded in FELIX laboratory using an AmaZon ion trap, compared to the one reported by Crestoni et *al.* at the CLIO facility in Orsay. Some spectral differences between $[P(H)]^+$ and $[P(O)H]^+$ are observed at 892 cm^{-1}, 1095 cm^{-1} and 1232 cm^{-1}, respectively where the stretching of the C–O and the bending of the COH related to the alcohol function are expected. Based on the spectral differences provided by IRMPD spectroscopy in Fig. 3.a, it can thus be inferred that the addition of an oxygen atom on Pro leads to the formation of a hydroxyl group in the pyrrolidine ring when hydroxyl radicals attack on the Pro moiety as previously observed [22]. A mixture of 3- and 4-hydroxyproline should be formed during the oxidation of Pro by gamma radiolysis in our experimental conditions. Diagnostic bands for the cis 3- and 4-hydroxyproline are observed at 1214 cm^{-1} and 1271 cm^{-1}, respectively. While cis 3-hydroxyproline exhibits a trough in dissociation yield at around 1214 cm^{-1} and a peak in yield at around 1271 cm^{-1}, the reverse is observed for cis 4-hydroxyproline [39].

The C–H bond in α position to the side-chain carboxylic group in

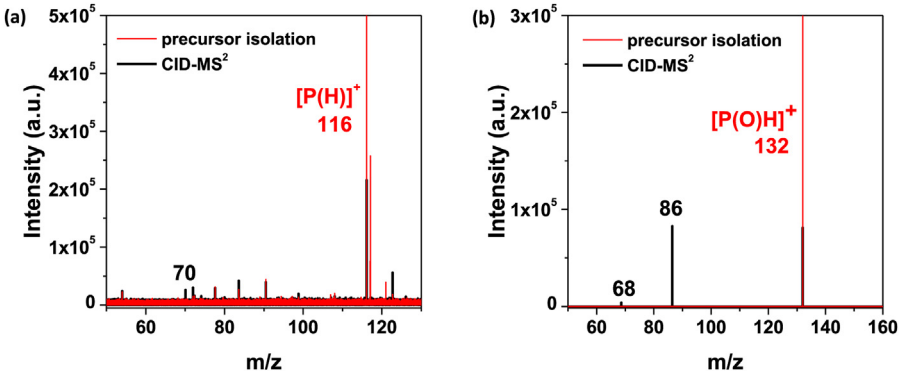

Fig. 2. CID-MS^2-fragmentation mass spectra of **(a)** $[P(H)]^+$ (*m*/*z* 116) and **(b)** $[P(O)H]^+$ (*m*/*z* 132).

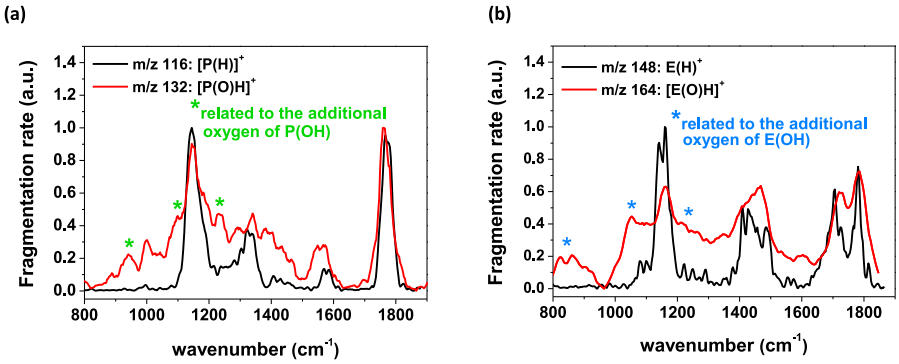

Fig. 3. Comparison between the IRMPD spectra of protonated non-oxidized amino acids (black) and protonated singly oxidized forms (red) for **(a)** Pro and (**b**) Glu.

glutamic acid represents the main site of the •OH radical attack leading to the formation of a hydroxylated residue [43]. Unfortunately, the CID-MS^2 fragmentation spectrum of [E(O)H]+ presents only one main fragment which corresponds to the loss of a water molecule, which is not diagnostic of the position of oxidation site on E. As shown in Fig. 3.b, the IRMPD spectrum of $[E(O)H]^+$ shows some extra bands at 855 cm^{-1}, 1050 and 1250 cm^{-1}, which can be assigned to the stretching mode of the C—O group of the alcohol function formed during the gamma radiolysis and the bending mode of the COH group. The C—O stretch shows up in the region 1260-1050 cm^{-1} [41], indicating the hydroxylation of E during gamma radiolysis while the position of this hydroxyl group still could not be identified according to the IRMPD spectrum.

The comparison of the experimental spectrum of $[P(O)H]^+$ with the calculated ones for the most stable structures of 3- and 4-hydroxyproline (**ProOH01_3** and **ProOH01_4**) are presented in Figure SI4. **ProOH01_3** is the singly oxidized form of the protonated proline with an additional 3-hydroxyl substituent. **ProOH01_4** has an additional hydroxyl group at the position 4 compared to protonated proline. **ProOH01_4** is 9.8 kJ mol^{-1} higher in energy compared to **ProOH01_3**. In the study of protonated proline reported by Wu et *al.* [40], although the experimental spectrum of protonated proline is most similar to the calculated spectrum of the structure with the lowest energy, the presence of higher conformers still could not be excluded. Likewise, both Acharya et *al.* and Crestoni et *al.* have shown that several low-lying conformations of hydroxyproline are populated simultaneously in the gas phase [39,42]. Since both **ProOH01_3** and **ProOH01_4** are in good agreement with the experimental spectrum of $[P(O)H]^+$ we can assume that it is possible to form 3- and 4-hydroxyproline in our experimental conditions. The protonation site is on the nitrogen atom for both **ProOH01_3** and **ProOH01_4**. They are stablized by an intramolecular hydrogen bond between the protonated amine group with the carbonyl oxygen. In **ProOH01_4**, the pyrrolidine ring adopts an *endo*-puckered configuration. **ProOH01_03** puckered in an *endo*-way as well.

The band assignments of $[P(O)H]^+$ are listed in Table SI3. The prominent band at 1147 cm^{-1} is assigned to a combination of CO and CN stretching along with NH_2, COH and CH_2 bending. The band at 1347 cm^{-1} corresponds to the CO and CN stretching accompanied by NH_2, COH and CH_2 bending modes. The weak band at 1561 cm^{-1} is ascribed to the scissoring mode of NH_2. The typical and intense band at 1762 cm^{-1} is assigned to the stretching of the carbonyl group.

The comparisons of the experimental spectrum of $[E(O)H]^+$ and the calculated ones for the most stable structures (**1-cc_4** and **1-cc_3**) are shown in Figure SI5. **1-cc_4** is more stable than **1-cc_3** of 5.2 kJ mol^{-1}. These two geometries are stabilized by two intramolecular interactions, NH···Oγ=C and NH···Oα=C ones. Both **1-cc_4** and **1-cc_3** are protonated on the amino nitrogen. **1-cc_4** has an additional hydroxy substituent at the position 4, compared to protonated glutamic acid. The hydroxyl substituent of **1-cc_3** is at the position 3.

The calculated spectra of these two geometries are quite similar. As already observed for $[P(O)H]^+$, both should be populated in our experimental conditions. Band assignements are listed in Table SI4 and they are obtained by comparing the calculated spectra of **1-cc_3** and **1-cc_4** with the experimental one.

The weak band centered at 855 cm^{-1} is assigned to a combination of CC stretching and CNH bending modes. The intense band at 1166 cm^{-1} is ascribed to the CO stretching and COH bending modes. The red-side shoulder at 1050 cm^{-1} is attributed to the

stretching of CO, CN and CC bonds. The small band at 1250 cm^{-1} is assigned to the stretching of CC bond and the bending of COH and CNH bonds. Another intense but less-resolved band at 1468 cm^{-1} is due to the combination of two calculated bands (1402 and 1494 cm^{-1} of **1-cc_3**; 1393 and 1495 cm^{-1} of **1-cc_4**) and assigned to the CO stretching, COH, NH_3 and CH_2 bending modes. A weak band at 1604 cm^{-1} is attributed to the waggling of NH_3. Two prominent bands at 1730 and 1786 cm^{-1} are attributed to the stretching mode of C═Oγ and C═Oα (C═Oα refers to the one located at the end of the alkyl chain while C═Oγ is the one on the other end), respectively. In conclusion, a mixture of the 3- and 4-isomers of hydroxyproline and hydroxy glutamic acid are identified as the +16 Da increment products of Pro and Glu after radiolysis-induced oxidation.

3.1. Met-Pro and Pro-Met

The mass spectra of the non-irradiated and irradiated dipeptides in a N_2O atmosphere are shown in Figure SI6. All observed species are listed and assigned in Table SI5.

The ion at *m/z* 247 is assigned to $[MP(H)]^+$ or $[PM(H)]^+$. Oxidation products can be observed by comparison of the mass spectra of the reference solutions and the irradiated ones. In the irradiated MP solution various products are observed. Oxidation processes are: dehydrogenation (*m/z* 245, -2 Da), decarboxylation (*m/z* 203, -44 Da), alone or along with dehydrogenation, (*m/z* 201; −46 Da), mono- or di-oxygenation, *m/z* 263 (+16 Da) and *m/z* 279 (+32 Da), eventually combined with hydrogen loss (*m/z* 261; +14 Da). In the irradiated PM solution, similar processes were observed although the decarboxylation process was less abundant. These products are in agreement with the results already observed by Bobrowski et *al.* [11,28], by pulse radiolysis, indicating that methionine oxidation triggers the reaction. Assuming that the intensities of the peaks observed in MS spectra are roughly proportional to the abundance of the compounds in the solution, the relative yields of radiolysis products are different for MP and PM. PM tends to undergo dehydrogenation (−2 Da) after the addition of an O-atom, yielding an ion at *m/z* 261, while the yield of this process is relatively low in MP.

The CID-MS^2 results of the principal radiation products observed in mass spectra of MP and PM are listed in Table SI6 and SI7 accompanied by assignments, respectively. The corresponding CID-MS^2 spectra are shown in Fig. 4 (+16 and +32 Da) and Figure SI7 and **SI8**.

The fragmentation pathways are quite similar in non-oxidized MP and PM. CID-MS^2 results confirm in both cases that Met and Pro side chains kept unmodified in the reference solutions. As for oxidation products, oxygen additions seem to be only localized on the S-containing side chains for singly and doubly oxidized compounds. $[MP(O)_2H]^+$ at *m/z* 279 shows two main fragments at *m/z* 199 and 181, respectively. They result from the loss of HSO_2CH_3 (−64 Da) and a combined process of dehydration (−18 Da) and loss of HSO_2CH_3 (−64 Da), respectively. The diagnostic fragment at *m/z* 197 of $[PM(O)_2H]^+$ results from a combined process of dehydrogenation (−2 Da) and loss of HSO_2CH_3 (−64 Da). These results prove that O-atom additions occurred only on S-containing side chains of Met residues and formed sulfoxide or sulfone groups.

The IRMPD spectra of protonated MP and PM (*m/z* 247) have been recorded and compared with the spectra of the oxidation products (*m/z* 263) in Fig. 5.

Several bands are observed in the IRMPD spectrum of $[MP(H)]^+$ (Fig. 5.a, black): 1138 cm^{-1} (intense), 1246 cm^{-1} (weak), 1432 cm^{-1} (intense), 1678 cm^{-1} (medium) and 1750 cm^{-1} (medium). Based on the previous studies of protonated Pro [40] and Met [44], IRMPD bands of $[MP(H)]^+$ can be assigned. The prominent band at 1138 cm^{-1} is attributed to the hydroxyl bending vibration. The weak band at 1246 cm^{-1} and the intense band centered at 1432 cm^{-1} correspond to CH, NH_2 and COH bending modes. Two bands observed at 1678 and 1750 cm^{-1} can be assigned to the amide I and the stretching mode of the C═O group, respectively.

In the spectrum of $[MP(O)H]^+$, an additional band centered at 994 cm^{-1} is observed. This band is characteristic of the S═O stretching mode [45]. The presence of this band is consistent with CID-MS^2 results and indicates that the +16-increment mass product MP(O) is ascribed to the formation of a sulfoxide group in methionine side chain. The intense band at 1140 cm^{-1} is assigned to the COH bending mode. The envelope of bands at 1239 cm^{-1} (weak), 1137 cm^{-1} (weak) and 1437 cm^{-1} (intense) is composed of CH, CH_2, NH_2 and COH bending modes. Two intense bands centered at 1666 and 1754 cm^{-1} originate from the stretch of two different carbonyl groups in Met and Pro moiety.

The comparison of IRMPD spectra of protonated non-oxidized PM with its oxidation products is reported in Fig. 5.b. Major observed bands of $[PM(H)]^+$ are: 1147 cm^{-1} (intense), 1249 cm^{-1} (medium), 1321 cm^{-1} (medium), 1540 cm^{-1} (medium), 1702 cm^{-1} (medium) and 1777 cm^{-1} (medium).

The strong absorbance at 1147 cm^{-1} is attributed to the COH bending mode. The less-resolved envelope of bands 1249 and 1321 cm^{-1} is composed of several CH and COH bending modes. The medium band centered at 1540 cm^{-1} is ascribed to NH bending mode in protonated PM. The bands at 1702 cm^{-1} and 1777 cm^{-1} are assigned to the amide I band and the stretching mode of the carbonyl group.

In the case of oxidized PM, a sulfoxide group is also formed, as already revealed by the CID-MS^2 results. In the spectrum of $[PM(O)H]^+$, the following bands are observed at: 1033 (intense, with a shoulder at 950 cm^{-1}), 1101 (medium), 1155 (medium), 1299 (medium), 1377 (medium), 1517 (medium), 1595 (weak), 1699 (intense) and 1769 (intense) cm^{-1}. The strong band at 1033 cm^{-1} with a shoulder at 950 cm^{-1} matches with the diagnostic sulfoxide stretching mode; the medium bands at 1101, 1155, 1299 and 1377 cm^{-1} are in the region of hybrid vibrational modes of CH, CH_2, COH bending; the bands at 1517 and 1595 cm^{-1} may correspond to the bending of NH; the remaining two absorption bands at 1699 and 1769 cm^{-1} are associated with the amide I and the stretching of the carbonyl group of the acid function.

3.2. Met-Pro-Met, Met-Pro-Pro-Met

The mass spectra of non-irradiated and irradiated peptides in a N_2O atmosphere for MPM and MPPM are reported in Figure SI9.

Radiolysis-induced products of MPM and MPPM are summarized in Table SI8. The main peaks observed in the mass spectra of non-irradiated samples correspond to the protonated molecules: $[MPM(H)]^+$ (*m/z* 378 in Figure SI9.a) and $[MPPM(H)]^+$ (*m/z* 475 in Figure SI9.b). The main oxidation products for MPM are observed at *m/z* 332 (−46 Da, loss of CO_2 and H_2), *m/z* 394 (+16 Da, addition of one O-atom) and *m/z* 410 (+32 Da, addition of two O-atoms), respectively. MPPM shows products at *m/z* 429 (loss of CO_2 and H_2), *m/z* 431 (loss of CO_2), *m/z* 491 (+16 Da, addition of one O-atom) and *m/z* 507 (+32 Da, addition of two O-atoms).

The CID-MS^2 spectra of $[MPM(H)]^+$, $[MPPM(H)]^+$ are shown in Figure SI10.Figure SI10. The CID-MS^2 spectra of their oxidized forms are reported in Fig. 6 Figure SI10-11. The assignments of the most intense peaks observed in the MS^2-CID spectra are reported in Table SI9 and SI10, respectively.

MPM and MPPM have two S-containing side chains susceptible to be oxidized. Compared to the loss of $HSCH_3$ (−48 Da) observed from $[MPM(H)]^+$, the $HSOCH_3$ (−64 Da) lost from $[MPM(O)H]^+$ suggests that the addition of one O atom during gamma radiolysis

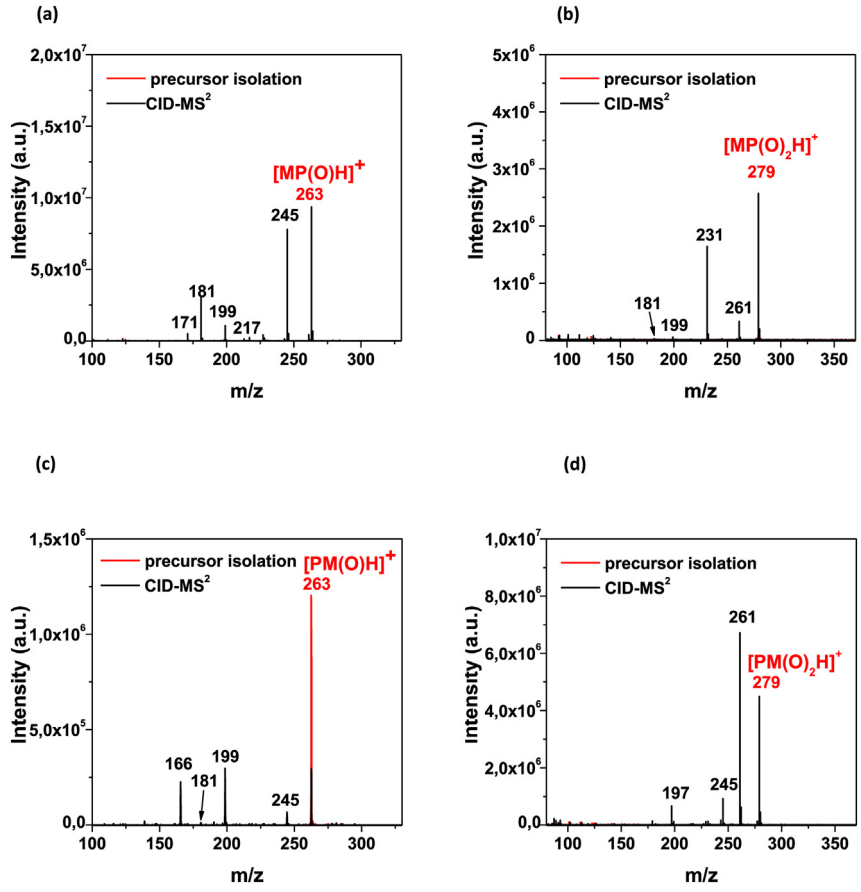

Fig. 4. CID-MS^2-fragmentation mass spectra of **(a)** $[MP(O)H]^+$ (*m/z* 263), **(b)** $[MP(O)_2H]^+$ (*m/z* 279), **(c)** $[PM(O)H]^+$ (*m/z* 263) and **(d)** $[PM(O)_2H]^+$ (*m/z* 279).

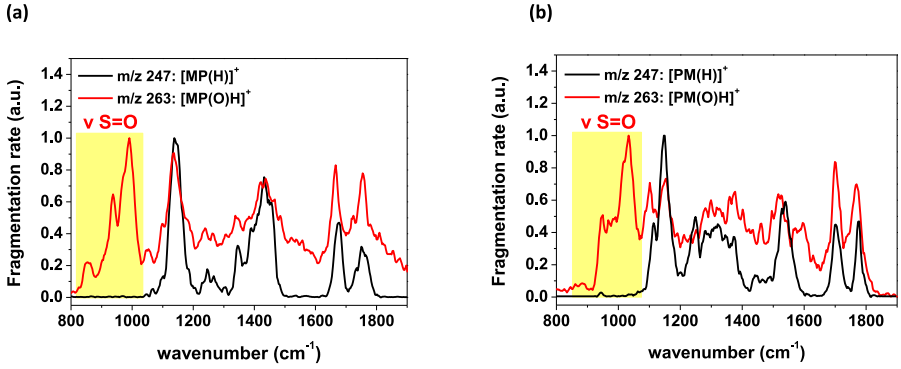

Fig. 5. Comparison between the IRMPD spectra of protonated non-oxidized peptides (black) and protonated singly oxidized forms (red) for MP **(a)** and PM (**b**).

oxidation in N_2O atmosphere can occur on the side chain of the Met moiety to form a sulfoxide group. Due to the simultaneous appearance of certain fragments, such as the one at *m/z* 263 (fragment y_2 with one added O-atom) and at *m/z* 245 (fragment b_2 with one added O-atom), we can conclude that the oxygen atom can be added to both N and C terminal Met side chains. The formation of the hydroxyproline during the gamma radiolysis of MPM by tandem mass spectrometry cannot be excluded, even if we did not observe the loss of two successive H_2O molecules that is diagnostic of the presence of hydroxyproline formation.

The double oxidized product $[MPM(O)_2H]^+$show the simultaneous fragments at *m/z* 362 corresponding to the loss of $HSCH_3$ (−46 Da) and at *m/z* 346 corresponding to the loss of $HSOCH_3$ (−64 Da) along with the absence of the fragment corresponding to the loss of HSO_2CH_3 (−80 Da). These results suggest that only one O-atom is added to the Sulphur one of the methionine side chain leading to the formation of a sulfoxide group. In addition, the key fragment at *m/z* 374, assigned to the loss of two water molecules, should reveal that the second O-atom is added to the Pro moiety forming a hydroxyl group.

MPPM owns one more Pro residue to separate the two Met residues located on the N and C terminal Met. Similar to MPM, the +16 mass increment products of MPPM can result from oxygen addition to Sulphur atom or formation of hydroxyproline, which is

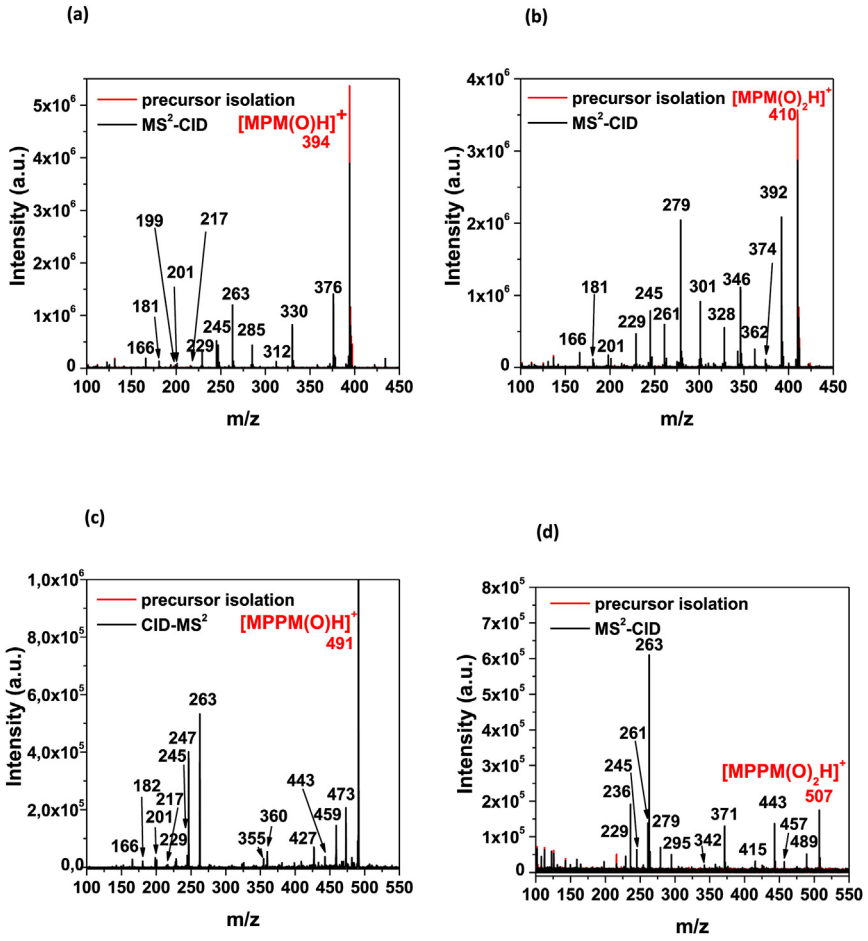

Fig. 6. CID-MS^2 fragmentation mass spectra of **(a)** $[MPM(O)H]^+$ (*m/z* 394), **(b)** $[MPM(O)_2H]^+$ (*m/z* 410), **(c)** $[MPPM(O)H]^+$ (*m/z* 491) and **(d)** $[MPPM(O)_2H]^+$ (*m/z* 507).

suggested by the presence of fragments at *m/z* 263 (fragment y_2 with one added O-atom) and *m/z* 245 (fragment b_2 with one added O-atom). Meanwhile, because of the simultaneous presence of two side chains of Met, the addition of the oxygen on Sulphur atom can be on either side of MPPM, C or N terminal.

The +32 mass increment products of MPPM also possess a mix of different sulfoxide products, revealed by the presence of the fragments at *m/z* 279 (fragment y_2 with two added O-atoms), *m/z* 263 (fragment y_2 with single added O-atom), *m/z* 261 (fragment b_2 with two added O-atoms) and *m/z* 245 (fragment b_2 with single added O-atom). No loss of HSO_2CH_3 has been observed, which makes it plausible to infer that no sulfone product has been formed. Interestingly, due to the presence of the *m/z* 229 peak which corresponds to the b_2 fragment, we can conclude that the +32 mass increment products of MPPM are ascribed to a combined hydroxyproline and sulfoxide product formation.

The IRMPD spectra of $[MPM(H)]^+$ (*m/z* 378), $[MPPM(H)]^+$ (*m/z* 475) and of their oxidation products with a *m/z* of +16 and +32 Da higher, are presented in Fig. 7 (**a** and **b**).

$[MPM(H)]^+$, $[MPPM(H)]^+$ and their oxidation products, show similar IRMPD spectra. The intense band at around 1150 cm^{-1} may be assigned to the COH bending mode. Absorbance in the middle fingerprint region leads to a combination of CH or NH bending vibrational modes. A band of increasing intensity at 1100 cm^{-1} is observed in the spectrum of +32 Da products compared to the non-oxidized form, indicating the probable hydroxylation of the proline. However, it is not possible to clearly identify the band associated with this functional group in the spectrum of the tripeptide that shows several bands in the congested fingerprint energy region.

The spectral signature of sulfoxide is the band located at 1020 cm^{-1} assigned to the sulfoxide stretching mode. This band is still present in the spectrum of M+32 product, even if its intensity is reduced. As shown in the CID-MS^2 results, the +32 mass increment products of MPM and MPPM correspond to a mixture of sulfoxide products and hydroxyproline while the +16 mass increment products are assigned exclusively to the sulfoxide products. The decrease of the intensity of the S═O band in doubly oxidized products supports the evidence that only a fraction of the addition of oxygen atoms has been converted to sulfoxide groups, different from the case in singly oxidized products where all the additional oxygen atoms were attached to Sulphur one to form sulfoxide products. Similar results have been observed in MM dipeptide by Ignasiak et *al.* [46]. Interestingly, the diagnostic band of the sulfoxide functional group is more intense in the spectrum of $[MPPM(O)_2H]^+$ compared to the spectrum of $[MPM(O)_2H]^+$, which indicates that the double oxidized product in MPPM should mainly be composed by a single oxidation on both methionine side chains. Previous study on transients formed during •OH-induced of Met-$(Pro)_n$-Met (n = 0–4) show the formation of transients stabilized by $(S \therefore S)^+$ and $(S \therefore O)^+$ bonds as well as the formation of a α-(alkylthio)alkyl radical (α-S) [15,47]. Furthermore, the yields of these transients depend on the number of Pro, although these yields do not depend in a simple way on the distance between methionine residues in the peptides. The amount of the $(S \therefore O)^+$ bound and αS radicals, in competition with the formation of the $(S \therefore S)^+$ bond, increases with the increasing of the number of prolines.

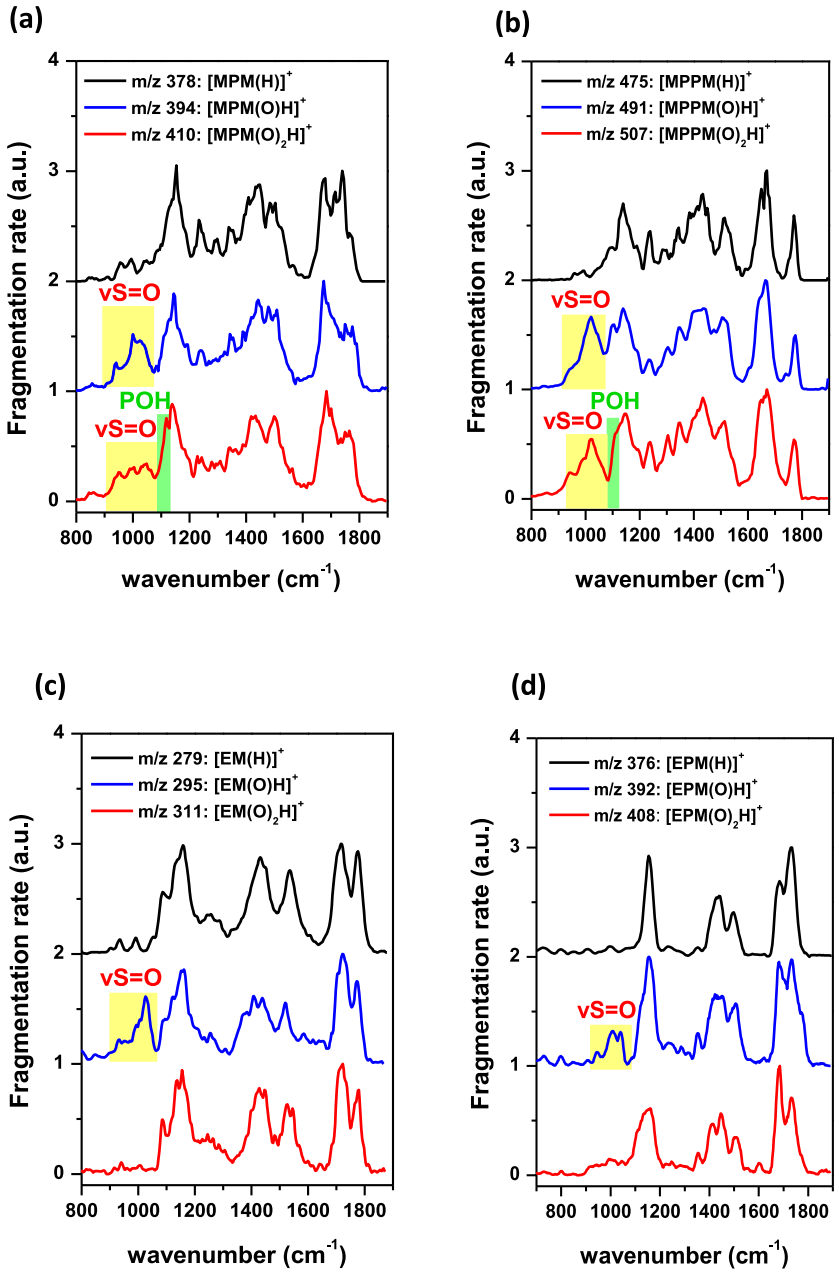

Fig. 7. Experimental IRMPD spectra of protonated non-oxidized and oxidized peptides. **(a)** IRMPD spectra of $[MPM(H)]^+$ at *m/z* 378 (black), $[MPM(O)H]^+$ at *m/z* 394 (blue) and $[MPM(O)_2H]^+$ at *m/z* 410 (red). **(b)** IRMPD spectra of the protonated $[MPPM(H)]^+$ at *m/z* 475 (black), $[MPPM(O)H]^+$ at *m/z* 491 (blue) and $[MPPM(O)_2H]^+$ at *m/z* 507 (red). **(c)** IRMPD spectra of the protonated $[EM(H)]^+$at *m/z* 279 (black), $[EM(O)H]^+$ at *m/z* 295 (blue) and $[EM(O)_2H]^+$ at *m/z* 311 (red). **(d)** IRMPD spectra of the protonated $[EPM(H)]^+$ at *m/z* 376 (black), $[EPM(O)H]^+$ at *m/z* 392 (blue) and $[EPM(O)_2H]^+$ at *m/z* 408 (red).

However, radiation chemical yields (G) of transients formed in MPM and MPPM are on the same order of magnitude, and both of them are controlled by the activated formation of the $(S\therefore S)^+$ bond. Little difference in the formation of transient species has been observed between MPM and MPPM [16], which confirms there is no direct link between the relative yields of different transient products and the yields of final products

These results seem also to confirm that the rate constant of oxidation of the methionine residue by OH radicals is larger compared to the proline residue and that some electron transfer between the amino acids residues should be possible at longer time scale, confirming the role of the methionine for long distance electron transfer. These preliminary results should be confirmed by the analysis of the final products of oxidation to be performed on MPPPM and MPPPPM peptides by tandem mass spectrometry and eventually IRMPD spectroscopy, even if the large size of peptides with 3 or 4 peptides could result in the observation of congested IRMPD spectra.

3.3. Glu-Met and Glu-Pro-Met

The mass spectra of non-irradiated and irradiated EM and EPM solutions in a N_2O atmosphere are shown in Figure SI11. Oxidation products +16 Da and +32 Da have been observed for both EM and

Table 1
Identified products in the mass spectra of the irradiated investigated systems.

Compound	Peaks observed in the MS *m/z*, z = 1	Identified products	Oxidation sites (Oxidized forms)
P	132	$[P(H)]^+ + O$	P(OH)
	148	$[P(H)]^+ + 2O$	$P(OH)_2$
E	164	$[E(H)]^+ + O$	E(OH)
MP	201	$[MP(H)]^+ - CO_2 - H_2$	–
	203	$[MP(H)]^+ - CO_2$	–
	245	$[MP(H)]^+ - H_2$	–
	261	$[MP(H)]^+ + O - H_2$	M(SO)
	263	$[MP(H)]^+ + O$	M(SO)
	279	$[MP(H)]^+ + 2O$	$M(SO_2)$
PM	201	$[PM(H)]^+ - CO_2 - H_2$	–
	245	$[PM(H)]^+ - H_2$	–
	261	$[PM(H)]^+ + O - H_2$	M(SO)
	263	$[PM(H)]^+ + O$	M(SO)
	279	$[PM(H)]^+ + 2O$	$M(SO_2)$
MPM	332	$[MPM(H)]^+ - CO_2 - H_2$	–
	394	$[MPM(H)]^+ + O$	M (SO)
	410	$[MPM(H)]^+ + 2O$	M(SO) + P(OH)
MPPM	429	$[MPPM(H)]^+ - CO_2 - H_2$	–
	431	$[MPPM(H)]^+ - CO_2$	–
	473	$[MPPM(H)]^+ - H_2$	–
	491	$[MPPM(H)]^+ + O$	M (SO) or P(OH)
	507	$[MPPM(H)]^+ + 2O$	M(SO) + P(OH)
EM	233	$[EM(H)]^+ - CO_2 - H_2$	–
	295	$[EM(H)]^+ + O$	M (SO)
	311	$[EM(H)]^+ + 2O$	$M(SO_2)$
EPM	330	$[EPM(H)]^+ - CO_2 - H_2$	–
	332	$[EPM(H)]^+ - CO_2$	–
	392	$[EPM(H)]^+ + O$	M (SO)
	408	$[EPM(H)]^+ + 2O$	$M(SO_2)$

EPM peptides as well as decarboxylation. The key transient α-aminoalkyl radicals (α N), formed after the loss of CO_2, were found to linearly decreased for γ-Glu-$(Pro)_n$-Met peptides when n increased from 0 to 2 [14]. However, there is no difference in the yield of the final product related to decarboxylation. Since the contact between the S-atom in the C-terminal Met residue and the N-atom of a deprotonated N-terminal amino group of Glu is controlled by the relative diffusion of the $S^{\bullet+}$ and the unoxidized N-atom, it is reasonable that the difference in the yield of decarboxylation can be small when the time scale is relatively large (for final products compared to transient ones).

The non-oxidized and oxidized ions with +16 Da and +32 Da oxo-forms were mass isolated from the solutions and investigated by CID-MS^2 in the FT-ICR mass spectrometry. The CID-MS^2 spectra are presented in Figure SI12-13 and fragment assignments are reported in Table SI11-12 for EM and EPM, respectively.

In the case of EM, the singly oxidized product EM(O) is obtained by the addition of one O-atom on the Sulphur one, which is evidenced by the fragment at *m/z* 213 identified with a successive loss of $HSOCH_3$ (−64 Da) and H_2O (−18 Da). For the doubly oxidized product $EM(O)_2$, the presence of a fragment at *m/z* 182 indicates that both oxygen atoms were added in the Met residue, leading to the formation of a sulfone.

As for EPM, the diagnostic fragment at *m/z* 166 of EPM(O) is assigned to y_1 fragment with one additional oxygen which indicates that oxidation occurs in the Met residue. The addition of one O-atom in the Met residue leads to sulfoxide product. The same fragment at *m/z* 182 has been observed for $EPM(O)_2$. Similar to $EM(O)_2$, two additional O-atoms located at Met part to form a sulfone in side chain.

The IRMPD spectra of protonated EM, EPM and protonated oxo-forms are shown in Fig. 7 (**c** and **d**). From non-oxidized species to singly oxidized product, the diagnostic feature at around 1000 cm^{-1} can be found for both $[EM(O)H]^+$ and $[EPM(O)H]^+$. When one Met residue is replaced by a Glu residue, the nature of the singly oxidation product does not change, but the doubly oxidation product leads to the formation of a sulfone, indicating that the glutamic acid is not oxidized in the presence of the methionine. The sulfoxide stretching mode for $[EM(O)H]^+$ and $[EPM(O)H]^+$ has been observed at 1020 cm^{-1}. The IRMPD spectrum of EPM shows bands at 1158 (intense, 1154 cm^{-1} for EPM(O)), 1257 (weak, 1244 cm^{-1} for EPM(O)), 1431 (intense, 1439 cm^{-1} for EPM(O)), 1536 (medium, 1499 cm^{-1} for EPM(O)), 1716 (intense, 1684 cm^{-1} for EPM(O)) and 1776 (intense, 1735 cm^{-1} for EPM(O)) cm^{-1}. The intense band at around 1155 cm^{-1} can be attributed to COH bending mode. The weak band at around 1250 cm^{-1} may corresponds to CC stretching along with COH and CNH bending modes. Bands at around 1430 and 1500 cm^{-1} are assigned to NH and CH bending modes. Two sharp prominent bands at around 1700 and 1750 cm^{-1} are assigned to the amide I band and the stretching mode of the carbonyl group, respectively. The +32 product for EM and EPM is a sulfone. The diagnostic band of the sulfone cannot be easily identified in the congested IRMPD spectra of the di- and tripeptides in the fingerprint region. Interestingly, no oxidation occurs on the E amino acid when it is in N terminal position both on the di- and tri-peptide.

4. Conclusions

In this work, the oxidation of a series of peptides containing Met and Pro residues has been investigated by using γ-radiolysis in the presence of N_2O to generate oxidizing $^{\bullet}OH$ radicals in aqueous solution. The structure of the final products has been systematically explored by tandem mass spectrometry and IRMPD spectroscopy, in order to get insight into the effect of the neighboring groups on their final oxidation products. Observed products are summarized

in Table 1.

Decarboxylation (−44 Da), dehydrogenation (−2 Da), combined loss of CO and H_2 (−46 Da), addition of one or two O-atoms (+16 Da or +32 Da) [44,48] are the main oxidation products obtained after γ radiolysis in water. A combination of O-addition and dehydrogenation was observed in MP and PM and in both peptides, proline is not oxidized. The yields of different processes strongly depend on the sequence of the amino acids: compared to PM, MP is more likely to undergo decarboxylation and less likely to be dehydrogenated. Interestingly, decarboxylation was not observed in oxidation of proline amino acid in solution, which indicates that the presence of methionine is necessary for this process to occur.

As for in MP_nM (n = 1 or 2) solutions, final γ-radiolysis products do not exhibit a significant difference when the number of inserted Pro increased from 0 to 2, despite the fact that the free radicals were different [11,12,28]. Again, we confirm that all Sulphur-centered free radicals lead to the same products whatever their 2c-3e bond. CID-MS^2 fragmentation spectra confirmed the assignment of products mentioned above and helped to localize the modified reaction sites. IRMPD spectra allowed us to gain further information about these modifications. The IRMPD spectral signature of the sulfoxide function at 1000 cm^{-1} reported previously [45] has been found in +16 Da oxidation products, confirming the formation of sulfoxide group and the use of this band as a spectroscopic tool to reveal the oxidation of methionine in peptides. However, a major point is that oxidation concerns also the proline residue although this residue is surrounded by 2 Met and no transient radical centered on Pro was observed in pulse radiolysis studies [15,47]. Two mechanisms can be proposed: i) direct H extraction from OH radicals despite the fact that the rate constant of OH radical attack on Pro is smaller than that of Met and that there are two Met residues. An attack by one of the two Met residues should be more probable. ii) oxidation of Pro might be initiated by electron transfer from Met free radical. An electron transfer at longer time scale has already been observed in the oxidation of Met-Trp dipeptide [48].

The change in distance between two Met residues (the number of inserted Pro from 0 to 2) in peptides did not cause a dramatic modification in the IRMPD spectra in the fingerprint region. Substitution of one Met residue by a Glu residue did not alter the identity of +16 Da product. The oxidation of Glu is never observed in the +32 Da product, contrary to Pro.

Declaration of competing interest

The authors declare that they have no known competing financial interests or personal relationships that could have appeared to influence the work reported in this paper.

Data availability

Data will be made available on request.

Acknowledgment

The research leading to these results has received funding from LASERLAB-EUROPE (grant agreement no. 871124, European Union's Horizon 2020 research and innovation programme). We gratefully acknowledge the Nederlandse Organisatie voor Wetenschappelijk Onderzoek (NWO) for the support of the FELIX Laboratory. Financial support from the French IR INFRANALYTICS FR2054 for conducting the research in Orsay MS/IRMPD platform is gratefully acknowledged.

B. Redlich and the FELIX laboratory are gratefully acknowledged. We thank the FELIX Laboratory technical staffs, in particular, Victor Claessen, Marije Barel, Wouter Stumpel and Bryan Willemsen for their efficient assistance during the IRMPD experiments. DS thanks Erna Gouwens from FELIX office for her assistance.

Appendix A. Supplementary data

Supplementary data to this article can be found online at https://doi.org/10.1016/j.ijms.2023.117029.

References

[1] S.H. Gellman, On the role of methionine residues in the sequence-independent recognition of nonpolar protein surfaces, Biochemistry 30 (1991) 6633–6636.
[2] J.C. Aledo, Methionine in proteins: the Cinderella of the proteinogenic amino acids, Protein Sci. 28 (2019) 1785–1796.
[3] S. Varadarajan, J. Kanski, M. Aksenova, C. Lauderback, D.A. Butterfield, Different mechanisms of oxidative stress and neurotoxicity for Alzheimer's Aβ(1–42) and Aβ(25–35), J. Am. Chem. Soc. 123 (2001) 5625–5631.
[4] D.A. Butterfield, beta-Amyloid-associated free radical oxidative stress and neurotoxicity: implications for Alzheimer's disease, Chem. Res. Toxicol. 10 (1997) 495–506.
[5] D.A. Butterfield, J. Kanski, Methionine residue 35 is critical for the oxidative stress and neurotoxic properties of Alzheimer's amyloid beta-peptide 1-42, Peptides 23 (2002) 1299–1309.
[6] E.R. Stadtman, H. Van Remmen, A. Richardson, N.B. Wehr, R.L. Levine, Methionine oxidation and aging, Biochim. Biophys. Acta 1703 (2005) 135–140.
[7] E.R. Stadtman, J. Moskovitz, R.L. Levine, Oxidation of methionine residues of proteins: biological consequences, Antioxidants Redox Signal. 5 (2003) 577–582.
[8] D.J. Bigelow, T.C. Squier, Thioredoxin-dependent redox regulation of cellular signaling and stress response through reversible oxidation of methionines, Mol. Biosyst. 7 (2011) 2101–2109.
[9] R.L. Levine, B.S. Berlett, J. Moskovitz, L. Mosoni, E.R. Stadtman, Methionine residues may protect proteins from critical oxidative damage, Mech. Ageing Dev. 107 (1999) 323–332.
[10] K.O. Hiller, B. Masloch, M. Goebl, K.D. Asmus, Mechanism of the hydroxyl radical induced oxidation of methionine in aqueous solution, J. Am. Chem. Soc. 103 (1981) 2734–2743.
[11] K. Bobrowski, C. Schöneich, J. Holcman, K.-D. Asmus, ȮH radical induced decarboxylation of methionine-containing peptides. Influence of peptide sequence and net charge, J. Chem. Soc., Perkin Trans. 2 (1991) 353–362.
[12] K. Bobrowski, G.L. Hug, D. Pogocki, B. Marciniak, C. Schöneich, Stabilization of sulfide radical cations through complexation with the peptide bond: mechanisms relevant to oxidation of proteins containing multiple methionine residues, J. Phys. Chem. B 111 (2007) 9608–9620.
[13] P. Filipiak, K. Bobrowski, G.L. Hug, D. Pogocki, C. Schöneich, B. Marciniak, formation of a three-electron sulfur-sulfur bond as a probe for interaction between side chains of methionine residues, J. Phys. Chem. B 120 (2016) 9732–9744.
[14] P. Filipiak, K. Bobrowski, G.L. Hug, C. Schöneich, B. Marciniak, N-terminal decarboxylation as a probe for intramolecular contact formation in γ-glu-(pro)n-met peptides, J. Phys. Chem. B 124 (2020) 8082–8098.
[15] P. Filipiak, K. Bobrowski, G.L. Hug, D. Pogocki, C. Schöneich, B. Marciniak, formation of a three-electron sulfur-sulfur bond as a probe for interaction between side chains of methionine residues, J. Phys. Chem. B 120 (2016) 9732–9744.
[16] G.V. Buxton, C.L. Greenstock, W.P. Helman, A.B. Ross, Critical Review of rate constants for reactions of hydrated electrons, hydrogen atoms and hydroxyl radicals (•OH/•O− in Aqueous Solution, J. Phys. Chem. Ref. Data 17 (1988) 513–886.
[17] R.A. Malak, Z. Gao, J.F. Wishart, S.S. Isied, Long-range electron transfer across peptide bridges: the transition from electron superexchange to hopping, J. Am. Chem. Soc. 126 (2004) 13888–13889.
[18] E. Karna, L. Szoka, T.Y.L. Huynh, J.A. Palka, Proline-dependent regulation of collagen metabolism, Cell. Mol. Life Sci. 77 (2020) 1911–1918.
[19] A.K. Mishra, J. Choi, E. Moon, K.-H. Baek, Tryptophan-rich and proline-rich antimicrobial peptides, Molecules 23 (2018) E815.
[20] G.-C. Zhou, Z. Weng, X. Shao, F. Liu, X. Nie, J. Liu, D. Wang, C. Wang, K. Guo, Discovery and SAR studies of methionine-proline anilides as dengue virus NS2B-NS3 protease inhibitors, Bioorg. Med. Chem. Lett. 23 (2013) 6549–6554.
[21] A. Mollica, M.P. Paradisi, K. Varani, S. Spisani, G. Lucente, Chemotactic peptides: fMLF-OMe analogues incorporating proline–methionine chimeras as N-terminal residue, Bioorg. Med. Chem. 14 (2006) 2253–2265.
[22] J. Kopoldová, M. Vorácek-Hübsch, Gamma-radiolysis of aqueous solution of proline, Z. Naturforsch. C Biosci. 30 (1975) 474–477.
[23] E.R. Stadtman, Oxidation of free amino acids and amino acid residues in proteins by radiolysis and by metal-catalyzed reactions, Annu. Rev. Biochem. 62 (1993) 797–821.
[24] E.R. Stadtman, R.L. Levine, Free radical-mediated oxidation of free amino acids and amino acid residues in proteins, Amino Acids 25 (2003) 207–218.
[25] J.E. Taylor, S.D. Bull, N-acylation reactions of amines, in: Comprehensive

Organic Synthesis II, Elsevier, 2014, pp. 427–478.
[26] M. Messerer, H. Wennemers, Reversing the enantioselectivity of a peptidic catalyst by changing the solvent, Synlett 2011 (2011) 499–502.
[27] E. Janata, R.H. Schuler, Rate constant for scavenging eaq- in nitrous oxide-saturated solutions, J. Phys. Chem. 86 (1982) 2078–2084.
[28] K. Bobrowski, C. Houée-Levin, B. Marciniak, Stabilization and reactions of sulfur radical cations: relevance to one-electron oxidation of methionine in peptides and proteins, CHIMIA International Journal for Chemistry 62 (2008) 728–734.
[29] A. Henglein, J.W.T. Spinks, in: R. J. Woods: an Introduction to Radiation Chemistry, third ed., John-Wiley and Sons, Inc., New York, Toronto, 1990. ISBN 0-471-61403-3. 574 Seiten, Preis: DM 91, 45., Ber. Bunsenges. Phys. Chem. 95 (1991) 451–451.
[30] S. Le Caër, Water radiolysis: influence of oxide surfaces on H2 production under ionizing radiation, Water 3 (2011) 235–253.
[31] J.M. Bakker, T. Besson, J. Lemaire, D. Scuderi, P. Maître, Gas-phase structure of a π-Allyl−Palladium complex: efficient infrared spectroscopy in a 7 T fourier transform mass spectrometer, J. Phys. Chem. 111 (2007) 13415–13424.
[32] D.J. Nesbitt, R.W. Field, Vibrational energy flow in highly excited molecules: role of intramolecular vibrational redistribution, J. Phys. Chem. 100 (1996) 12735–12756.
[33] J. Lemaire, P. Boissel, M. Heninger, G. Mauclaire, G. Bellec, H. Mestdagh, A. Simon, S.L. Caer, J.M. Ortega, F. Glotin, P. Maitre, Gas phase infrared spectroscopy of selectively prepared ions, Phys. Rev. Lett. 89 (2002), 273002.
[34] J. Oomens, A.J.A. van Roij, G. Meijer, G. von Helden, Gas-phase infrared photodissociation spectroscopy of cationic polyaromatic hydrocarbons, Astrophys. J. 542 (2000) 404–410.
[35] J. Martens, G. Berden, C.R. Gebhardt, J. Oomens, Infrared ion spectroscopy in a modified quadrupole ion trap mass spectrometer at the FELIX free electron laser laboratory, Rev. Sci. Instrum. 87 (2016), 103108.
[36] Y. Nosenko, F. Menges, C. Riehn, G. Niedner-Schatteburg, Investigation by two-color IR dissociation spectroscopy of Hoogsteen-type binding in a metalated nucleobase pair mimic, Phys. Chem. Chem. Phys. 15 (2013) 8171–8178.
[37] D. Oepts, A.F.G. van der Meer, P.W. van Amersfoort, The Free-Electron-Laser user facility FELIX, Infrared Phys. Technol. 36 (1995) 297–308.
[38] G. Berden, M. Derksen, K.J. Houthuijs, J. Martens, J. Oomens, An automatic variable laser attenuator for IRMPD spectroscopy and analysis of power-dependence in fragmentation spectra, Int. J. Mass Spectrom. 443 (2019) 1–8.
[39] B. Acharya, W.K.D.N. Kaushalya, J. Martens, G. Berden, J. Oomens, A.L. Patrick, A combined infrared ion spectroscopy and computational chemistry study of hydroxyproline isomers, J. Am. Soc. Mass Spectrom. 31 (2020) 1205–1211.
[40] R. Wu, T.B. McMahon, An investigation of protonation sites and conformations of protonated amino acids by IRMPD spectroscopy, ChemPhysChem 9 (2008) 2826–2835.
[41] A. Bouchet, J. Klyne, S. Ishiuchi, M. Fujii, O. Dopfer, Conformation of protonated glutamic acid at room and cryogenic temperatures, Phys. Chem. Chem. Phys. 19 (2017) 10767–10776.
[42] M.E. Crestoni, B. Chiavarino, D. Scuderi, A. Di Marzio, S. Fornarini, Discrimination of 4-hydroxyproline diastereomers by vibrational spectroscopy of the gaseous protonated species, J. Phys. Chem. B 116 (2012) 8771–8779.
[43] W.M. Garrison, Reaction mechanisms in the radiolysis of peptides, polypeptides, and proteins, Chem. Rev. 87 (1987) 381–398.
[44] M. Ignasiak, D. Scuderi, P. de Oliveira, T. Pedzinski, Y. Rayah, C. Houée Levin, Characterization by mass spectrometry and IRMPD spectroscopy of the sulfoxide group in oxidized methionine and related compounds, Chem. Phys. Lett. 502 (2011) 29–36.
[45] M. Ignasiak, D. Scuderi, P. de Oliveira, T. Pedzinski, Y. Rayah, C. Houée Levin, Characterization by mass spectrometry and IRMPD spectroscopy of the sulfoxide group in oxidized methionine and related compounds, Chem. Phys. Lett. 502 (2011) 29–36.
[46] M. Ignasiak, P. de Oliveira, C.H. Levin, D. Scuderi, Oxidation of methionine-containing peptides by OH radicals: is sulfoxide the only product? Study by mass spectrometry and IRMPD spectroscopy, Chem. Phys. Lett. 590 (2013) 35–40.
[47] P. Filipiak, K. Bobrowski, G.L. Hug, D. Pogocki, C. Schöneich, B. Marciniak, New insights into the reaction paths of 4-carboxybenzophenone triplet with oligopeptides containing N- and C-terminal methionine residues, J. Phys. Chem. B 121 (2017) 5247–5258.
[48] D. Scuderi, M.T. Ignasiak, X. Serfaty, P. de Oliveira, C.H. Levin, Tandem mass spectrometry and infrared spectroscopy as a tool to identify peptide oxidized residues, Phys. Chem. Chem. Phys. 17 (2015) 25998–26007.